

ONLINE MODELING OF THE RARE ISOTOPE REACCELERATOR - REA *

Walter Wittmer[†], Daniel Alt, Shannon Krause, Daniela Leitner, Samuel Nash, Randall Rencsok,
Jose Alberto Rodriguez, Michael Syphers, Xiaoyu Wu, NSCL, East Lansing, Michigan, USA

Abstract

With the installation and commissioning of the third accelerating cryomodule in summer of 2014 the first phase of the radioactive ion beams postaccelerator ReA[1] at National Superconducting Cyclotron Laboratory (NSCL) at Michigan State University (MSU) will be completed. ReA was integrated in 2013 into the Coupled Cyclotron Facility providing unique low-energy rare isotope beams. After the fast rare isotopes are stopped in a gas stopping system, mass separated and their charge state boosted in an Electron Beam Ion Trap (EBIT), the ions are reaccelerated in a compact superconducting (SC) LINAC. For rare isotope operations, the LINAC is pre-tuned using stable pilot beams with a similar mass to charge ratio as the rare isotope beams and consequently the system is scaled. Scaling steps of up to 5% are needed to change to the radioactive beams. To preserve the stringent beam characteristic on the experimental end station a precise online model is required. We will present the status of this online model.

INTRODUCTION

During the first commissioning experiments during summer of 2013 [2] and spring this year valuable experience has been gained for the future operation. Most noticeable the importance of an accurate online model describing the machine for the scaling of the beam line from the pilot beam to the radioactive ion beam (RIB) delivered to the experiments. Scaling of the beam lines has to be possible for a range of at least $\pm 5\%$, including magnets and superconducting cavities with constant and changing velocity.

Figure 1 depicts the layout of ReA. On the left the EBIT, low energy beam line and offline pilot source are depicted in dark green, followed by the four-rod RFQ (light green), rebunching (red) and accelerating (blue, yellow) cryomodules. The right shows the high-energy beam transport (HEBT) into the experimental hall and the experimental setups. During the previous commissioning a drift tube with two BPMs and a diagnostic box had been installed in the place of the last cryomodule.

Previously the optics of the HEBT had been measured and compared to the design model. Good agreement had been found as reported in [2]. The LEBT line is in the process of being reconfigured to improve its diagnostics capability and add bunching at a different frequency (16 MHz). These changes require a modified optics and therefore no

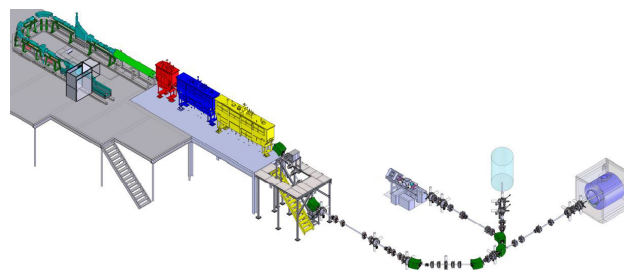


Figure 1: Layout of ReA3 with the final cryomodule (yellow) installed.

significant effort had been made to develop an accurate online model in this area.

Before shutting down for the installation of the third cryomodule this spring the first of a series of measurements were conducted to improve the understanding of the model in the LINAC area.

LAYOUT OF BEAM LINE AND EXPERIMENTAL SETUP

Two different ion species can be extracted from an offline ion source (LB-source) from which the molecular hydrogen H_2^+ beam was used for the measurement. In this setup the RFQ can be operated in CW mode. The beam is then focused by an electrostatic triplet and bent into the main beam line by a combination of 75° (spherical) and 15° (parallel plate) benders. Two doublets and a solenoid then focus the beam into the RFQ with the required injection energy of 12keV/u. The RFQ accelerates the beam to 600 keV/u, which is then injected into the SRF LINAC.

The first rebunching module comprises a single quarter wave cavity ($\beta = 0.041$) and two superconducting 9 Tesla solenoids with integrated steering magnets. The second accelerating module houses 6 cavities and 3 solenoids of the same type. Before, between and after each module a diagnostic box is installed. The first had temporarily a pepper pot emittance scanner installed for this measurement, to determine the initial condition before the SRF LINAC. The two following each have a Faraday cup and 45° slit drive installed to measure the beam profile, besides other diagnostics.

MEASUREMENTS

The aim of this measurement campaign was to understand the behavior of the beam optics in the SRF LINAC

* Work supported by Michigan State University

[†] wittmer@nscl.msu.edu

Content from this work may be used under the terms of the CC BY 3.0 licence (© 2014). Any distribution of this work must maintain attribution to the author(s), title of the work, publisher, and DOI.

without acceleration cavities. These were turned off during the measurements. The initial condition was measured with a DREBIT pepper pot installed in the diagnostic box before the rebunching cryo module. The transverse beam properties are fully determined with the emittance measurement at this location.

Emittance Measurement after RFQ

New analyzing software was developed for the emittance measurement using the MATLAB framework. It analyzes each imaged beamlet individually and reconstructs the emittance ellipse projections of the four dimensional emittance ellipsoid. The position coordinate and thereby its resolution is determined by the mask geometry of the pepper pot and therefore is determined by the device. The angle resolution can be increased by a fit over the beamlet projection and dividing it into angle dependent slices over which the intensity is integrated. Figure 2 shows the result of the emittance analysis for the horizontal plane. To eval-

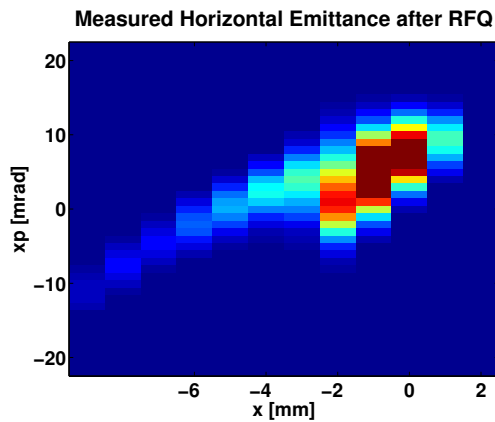


Figure 2: Reconstruction of the horizontal emittance measured with the pepper pot after the RFQ. The difference of the resolution of the angle and position coordinate is clearly visible. The tail is also visible in the simulation but it shows tails on both sides. The right tail is missing from the measurement as the beam exceeded the hole mesh.

uate the algorithm a Gaussian distribution was generated with DYNAC [3] based on the measured beam characteristic after the RFQ. This distribution was then analyzed again by the code and compared to the original input parameters as shown in table 1. An excellent agreement between ini-

Table 1: Benchmark Results for Emittance Code

Param.	Unit	Input	Output
α_x	1	-1.527	-1.525
α_y	1	-0.991	-0.990
β_x	mm	1.110	1.109
β_y	mm	0.583	0.583
ϵ_x	π mm mrad	7.059	7.069
ϵ_y	π mm mrad	7.376	7.383

tial and calculated parameter is found.

Part of the daily operations routine is to tune the RFQ amplitude optimizing beam transmission. To study the effect of this tuning on the transverse phase space the RFQ amplitude was changed in steps of 0.01 ($U_{rod} = 250 V$) from 1.59 ($U_{rod} = 39.1 kV$) to 1.79 ($U_{rod} = 44.1 kV$) units in the control system and the emittance recorded with the pepper pot. The result of this measurement is recorded in Fig. 3. The best transmission for this se-

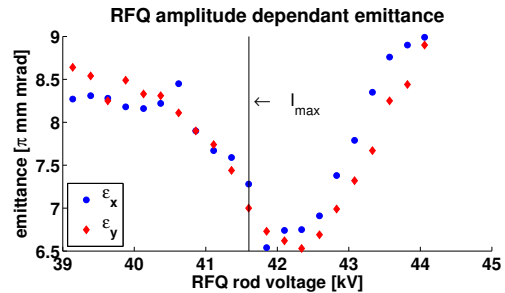


Figure 3: RFQ amplitude dependant emittance evolution measured with pepper pot after RFQ.

ries of measurements was recorded at an amplitude of $U_{rod I_{max}} = 41.6 kV$. This is lower than the setting optimized for the lowest emittance ($U_{rod \epsilon_x min} = 41.9 kV$, $U_{rod \epsilon_y min} = 42.1 kV$).

Beam Profile Measurements

The type of diagnostic installed between the SRF cryomodules is limited by the required cleanliness for the cavity surfaces. This does not permit to install a pepper pot to measure the emittance in these locations. The standard Faraday cup to measure the beam current and a 45° slit scanner allows sampling of the beam profile in the horizontal, vertical and one transverse 45° rotated direction. The latter allows inspecting the coupled beam characteristic but for a full evaluation an additional orthogonal slit would be needed. This is not possible as this slit's orientation would be located in the direction of the motion. Optimal beam transport has been achieved in the past by tuning round beam profiles at the diagnostic box locations. Figure 4 depicts the result of such a beam profile scan after

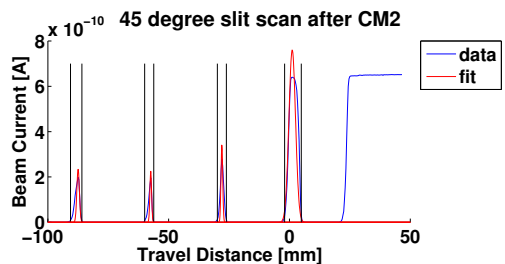


Figure 4: A 45° slit scan measurement after the second cryomodule.

the second module. The three peaks on the left show the vertical, skew and horizontal beam profile amplified by a

factor of $\sqrt{2}$. The right peak results from a 5 mm hole centered on the theoretical beam axis and the right shoulder is the beam current with the slit paddle not interfering with the beam. Hole peak and shoulder show equal intensity indicating a well centered beam smaller than 5mm. The results for both diagnostic box measurements are presented in table 2. The boundaries of the beam are determined by a

Table 2: Measured Beam Sizes with 5% Cutoff

Beam size	Unit	after Module 1	after Module 2
hor.	mm	4.0	2.7
ver.	mm	3.5	3.3

cutoff criterion, which in this particular case are 5% of the signal maximum, indicated by the black lines at both sides of each peak.

Comparison of Online Model to Measurements

The machine settings for the solenoids, saved in the control system, were translated to effective length and magnetic field by using the measured solenoid. Together with the measured initial beam conditions before the SRF LINAC an online model was generated for the LINAC and the simulated beam sizes compared to the measured. Figure 5 pictures the simulated contour plot with the overlaid beam measurement. The figure shows an excellent

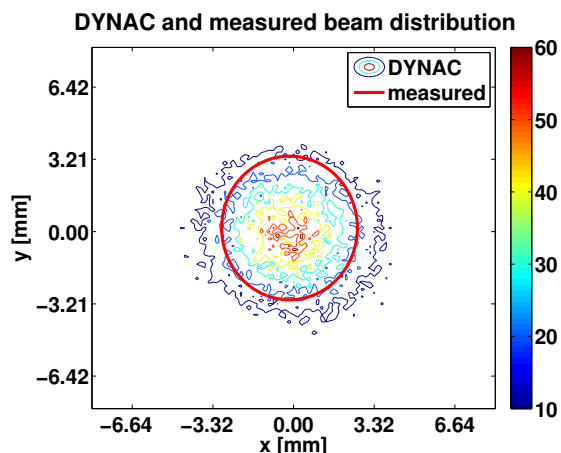


Figure 5: Contour plot of the simulated beam image in the location of the last beam diagnostic station overlaid with the ellipse constructed from the beam measurement. The ellipse indicates the beam size containing approx. 95 % of the beam.

tive agreement between measurement and simulation. The fluctuating noise floor between 1 and 5 pA creates an offset and during the profile scan (up to 3 minutes depending on number of steps) the beam jitters due to the source behavior. This makes a quantitative comparison of these numbers to the simulations very difficult.

The beam envelope has to be periodic in the SRF LINAC for optimized transmission. Figure 6 shows the simulated

progression of the beam envelope in this area based on the measured initial beam conditions after the RFQ and the control system set points for the solenoids. The envelope is

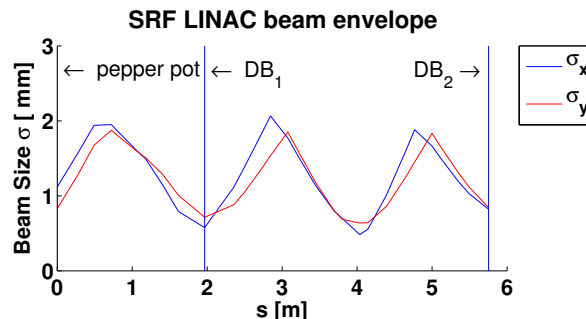


Figure 6: Simulated beam envelope in the SRF LINAC based on measured initial conditions and control system set points for solenoids.

practically ideal, showing waists at approx. 2 and 6 meters where the diagnostic boxes are located.

CONCLUSIONS AND OUTLOOK

Measurement of the RFQ-dependent emittance shows that the RFQ should not be tuned only by maximizing the transmission. Both emittance and transmission have to be used as figures of merit. The measured data set indicates that the optimized amplitude for both emittances and transmission are very similar.

The pepper pot measurement after the RFQ has proven very valuable to determine the beam condition entering the SRF LINAC. The current device uses an MCP to image the beamlets. The beam can penetrate the MCP plate with its relative high beam energy creating secondary electrons along its track, which could increase the beam size of the beamlets measured on the MCP phosphor. This would explain the larger emittance compared to the design values. To verify the measured emittance after the RFQ a pepper pot with a scintillating crystal for imaging will be developed and installed.

With the measured emittance after the RFQ an accurate online model was developed for the SRF LINAC without the SRF cavities. To complete the online model a dedicated measurement including the SRF cavities will be conducted as soon as the installation and commissioning of the last cryomodule is completed.

REFERENCES

- [1] D.Leitner, et al., "Status of the ReAccelerator facility ReA for rare isotopes.", FRYBA2, Proceedings of NA-PAC2013, Pasadena, CA, USA.
- [2] W.Wittmer, et al., "Results From the Linac Commissioning of the Rare Isotope Reaccelerator - ReA.", MOPSM07, Proceedings of NA-PAC2013, Pasadena, CA, USA.
- [3] E. Tanke, et al., "DYNAC: A multi-particle beam dynamics code for leptons and hadrons.", Gyeongju, TH429, p. 667 (2002).